Published online 24 August 2015 *Nucleic Acids Research, 2015, Vol. 43, No. 21* ***10227–10237***
doi: 10.1093/nar/gkv847

Histone variant H3.3 provides the heterochromatic H3 lysine 9 tri-methylation mark at telomeres

Maheshi Udugama[1], Fiona T. M. Chang[1], F. Lyn Chan[1], Michelle C. Tang[2], Hilda A. Pickett[3], James D. R. McGhie[1], Lynne Mayne[1], Philippe Collas[4], Jeffrey R. Mann[5] and Lee H. Wong[1,*]

[1]Department of Biochemistry and Molecular Biology, Monash University, Clayton, Victoria 3800, Australia, [2]Department of Zoology, University of Melbourne, Parkville, Victoria 3052, Australia, [3]Telomere Length Regulation Group, Children's Medical Research Institute, University of Sydney, Westmead, New South Wales, Australia, [4]Department of Molecular Medicine, Institute of Basic Medical Sciences, Faculty of Medicine, and Norwegian Center for Stem Cell Research, University of Oslo, 0317 Oslo, Norway and [5]Department of Anatomy and Developmental Biology, Monash University, Clayton, Victoria 3800, Australia

Received March 28, 2015; Revised July 7, 2015; Accepted August 11, 2015

ABSTRACT

In addition to being a hallmark at active genes, histone variant H3.3 is deposited by ATRX at repressive chromatin regions, including the telomeres. It is unclear how H3.3 promotes heterochromatin assembly. We show that H3.3 is targeted for K9 trimethylation to establish a heterochromatic state enriched in trimethylated H3.3K9 at telomeres. In *H3f3a*$^{-/-}$ and *H3f3b*$^{-/-}$ mouse embryonic stem cells (ESCs), H3.3 deficiency results in reduced levels of H3K9me3, H4K20me3 and ATRX at telomeres. The *H3f3b*$^{-/-}$ cells show increased levels of telomeric damage and sister chromatid exchange (t-SCE) activity when telomeres are compromised by treatment with a G-quadruplex (G4) DNA binding ligand or by ASF1 depletion. Overexpression of wild-type H3.3 (but not a H3.3K9 mutant) in *H3f3b*$^{-/-}$ cells increases H3K9 trimethylation level at telomeres and represses t-SCE activity induced by a G4 ligand. This study demonstrates the importance of H3.3K9 trimethylation in heterochromatin formation at telomeres. It provides insights into H3.3 function in maintaining integrity of mammalian constitutive heterochromatin, adding to its role in mediating transcription memory in the genome.

INTRODUCTION

Chromatin is organized into biochemically and functionally distinct domains, which are marked by enrichment in combinations of canonical histones and histone variants. Substitution of one or more of the canonical histones with corresponding histone variant(s) by specific chaperones exerts considerable influence on the structure and function of chromatin, including the regulation of transcription and epigenetic memory (1,2). In eukaryotes, the histone variant H3.3 is distinct from canonical H3.1 and H3.2 in that H3.3 is expressed at all stages of the cell cycle and can be incorporated into chromatin independently of DNA replication. In contrast, H3.1 and H3.2 are expressed only during S phase and incorporated into chromatin by the chaperone CAF1 only during DNA replication. H3.3 is loaded mainly at actively transcribed sites by H3.3-specific chaperone HIRA (3). At these sites, H3.3 is associated with marks linked to active chromatin such as H3 lysine 4 trimethylation (4,5) and H3.3 deposition at these sites is required to maintain the epigenetic memory of an active state in the absence of transcription (6) and promote an open chromatin conformation for the binding of transcription factors and co-factors to activate transcription (7).

Besides being a mark of active genes, H3.3 is loaded by the ATRX/DAXX chaperone complex to heterochromatic regions, which includes telomeres and pericentric heterochromatin (8–15). The importance of H3.3 and ATRX in chromatin repression is implied by recent studies showing a strong linkage between ATRX mutations and the Alternative Lengthening of Telomeres phenotype (ALT; ATRX is mutated ∼90% of ALT cancers) in telomerase-negative human cancers, which maintain telomere length via homologous recombination-mediated telomere extension (16–25). It is unclear how ATRX mutations drive telomere dysfunction and cancer development. A recent study shows that ATRX binds genomic sites that are prone to form a four-stranded secondary structure known as G-quadruplex (G4) DNA, and which include the G-rich telomeric DNA (14). A proposed model is that the formation of G4 DNA may perturb replication and ATRX-mediated loading of H3.3 is required to re-chromatinize the 'late-replicated telomeric DNA' (26,27). The absence of ATRX such as in ALT cancers may account for the failure to re-chromatinize telom-

*To whom correspondence should be addressed. Tel: +61 3 9902 4925; Fax: +61 3 9902 9500; Email: lee.wong@monash.edu

eric DNA, resulting in persistent replication stalling and in turn leading to DNA damage, ALT and genome instability (23). Many important questions remain unanswered from these postulations: for example, it is still unclear whether ATRX is recruited by G4 DNA at the telomeres although ATRX binding sites including the telomeres tend to form G4 structures. Another possible model is that ATRX may be recruited to load H3.3 as a response to nucleosomal loss caused by stalled replication or other similarly disruptive activities including transcription. This agrees with a recent study in *Drosophila* reporting that ATRX homolog *Xnp* directs H3.3 loading at nucleosome-depleted gaps formed at actively transcribed sites (28).

In this study, we define the role of H3.3 in facilitating the assembly of a normal heterochromatic state, which is critical for telomeric function (10–12,15). We show that H3.3 supply and loading are essential in order to provide the heterochromatic K9 trimethylation mark required to maintain chromatin repression at telomeres. In *H3f3a* and *H3f3b* null mouse embryonic stem cells (ESCs), H3.3 deficiency results in reduced levels of H3K9me3 level, H4K20me3 and ATRX at the telomeres, accompanied with an increase in telomeric transcription. After induction of replication stress or nucleosome disruption, these cells also suffer greater levels of DNA damage and t-SCE at telomeres. This compromised heterochromatic state at the telomere can be alleviated by an expression of a wild-type (WT) H3.3 but not a H3.3K9A mutant protein. We also demonstrate a stepwise mechanism whereby the histone methyltransferases (HMTases) including SETDB1 (ESET/KMT1E), SUV39H1 and SUV39H2 (KMT1A and KMT1B) promote the formation of the H3.3K9me3 mark at telomeres. Our results show the importance of H3.3 supply in promoting the assembly of a heterochromatic state critical for telomere function. We demonstrate that H3.3 at the telomeres is utilized as a heterochromatic mark, via trimethylation of its K9 residue. Our study provides insights into the role of H3.3 in controlling epigenetic inheritance at a constitutive heterochromatic domain.

MATERIALS AND METHODS

Cell culture

Mouse ESCs were cultured in Dulbecco's modified Eagle's medium supplemented with 15% heat-inactivated foetal calf serum, 10^3 units/ml leukemia inhibitory factor and 0.1 mM β-mercaptoethanol. *H3f3a*$^{-/-}$ and *H3f3b*$^{-/-}$ ESCs were generated in two rounds of targeting as described earlier (29,30). The Neomycin resistance gene cassette was removed by overexpression of Cre recombinase.

Antibodies

Antibodies used were directed against H3 (Abcam ab1791), H4 (Merck Millipore), H3.3 (Merck Millipore 09838), H3K9me1 (Abcam ab9045), H3K9me3 (Abcam ab8898), H4K20me3 (Abcam ab9053), ATRX (Santa Cruz Biotechnologies sc15408), DAXX (Santa Cruz Biotechnologies M112), SETDB1 (Cell Signaling), phosphorylated CHK2T68 (Cell Signaling), Tubulin (Roche), *myc* tag (Merck Millipore) and γH2A.X/phospho-histone H2A.X (Ser139) (Merck Millipore JBW301 and Biolegend 2F3).

Immunofluorescence analysis

Cells were treated with microtubule-depolymerizing agent Colcemid for 1 h at 37°C, harvested for hypotonic treatment in 0.075 M KCl, cytospun on slides and incubated in KCM buffer (a KCl based buffer for cytospun metaphase chromosome spreads; 120 mM KCl, 20 mM NaCl, 10 mM Tris.HCl at pH 7.2, 0.5 mM ethylenediaminetetraacetic acid (EDTA), 0.1% [v/v] Triton X-100 and protease inhibitor) (31). Slides were blocked in KCM buffer containing 1% BSA and incubated with the relevant primary and secondary antibodies for 1 h at 37°C. After each round of antibody incubation, slides were washed three times in KCM buffer. Slides were then fixed in KCM with 4% formaldehyde and mounted in mounting medium (Vetashield). Images were collected using a fluorescence microscope linked to a CCD camera system.

Telomere CO-FISH (Co-fluorescence *in situ* hybridization)

Cells were incubated for 16–20 h in fresh medium containing BrdU (10 μg/ml). An hour before harvesting, Colcemid was added to the media to accumulate mitotic cells. Cells were harvested and resuspended in 0.075 M KCl (prewarmed to 37°C). Ice-cold methanol-acetic acid (3:1 ratio) was added to cell suspension. The cell suspension was spun (5 min at 1000 rpm) and washed twice in methanol-acetic acid. Cells were dropped onto slides and allowed to dry overnight. Slides were rehydrated in 1× phosphate buffered saline (PBS) for 5 min at room temperature, incubated with 0.5 μg/ml RNaseA (in PBS, DNase free) for 10 min at 37°C and stained with 0.5 μg/ml Hoechst 33258 in 2× saline sodium citrate solution (SSC) for 15 min at room temperature. Subsequently, slides were placed in a shallow plastic tray, covered with 2× SSC and exposed to 365 nm ultraviolet light at room temperature for 45 min. The BrdU-substituted DNA strands were digested with at least 10 U/μl of Exonuclease III at room temperature for 30 min. Slides were washed in 1× in PBS, dehydrated in ethanol series 70, 95, 100% and air dried. FISH was performed by hybridization with Cy3/Cy5-conjugated telomere peptide nucleic acid (PNA) probe in 10 mM NaHPO4 pH 7.4, 10 mM NaCl, 20 mM Tris, pH 7.5 and 50% formamide. The slides were not subjected to DNA denaturation.

Chromatin immunoprecipitation (ChIP) and re-ChIP

Cells were harvested and crosslinked with 1% paraformaldehyde for 10 min at room temperature. For ATRX ChIP, cells were cross-linked first with 2 mM EGS (Pierce 26103) for 45 min then subsequently with 1% paraformaldehyde for 15 min. Excess formaldehyde was quenched with glycine at a final concentration of 0.25 M. Cell were washed with PBS, pelleted and lysed in cold cell lysis buffer (10 mM Tris pH 8, 10 mM NaCl, 0.2% NP40 and protease inhibitors). Nuclei were centrifugated and resuspended in 50 mM Tris pH 8, 10 mM EDTA and 1% sodium dodecyl sulphate (SDS), and sonicated with a Bioruptor (Diagenode) to obtain chromatin fragments of 500 bp or less. Resulted chromatin was diluted in dilution buffer (20 mM Tris pH 8, 2 mM EDTA, 150 mM NaCl, 1% Triton X-100 and 0.01% SDS and protease

inhibitors) and pre-cleared with Protein A sepharose beads at 4°C. Pre-cleared chromatin was immunoprecipitated with antibody-bound beads at 4°C overnight. For each ChIP reaction, 2–5 μg of antibody and 20 μl of Protein A Sepharose beads (50% slurry) were used. The immunoprecipitated material was washed and eluted in 100 mM $NaHCO_3$ and 1% SDS. The eluted material was treated with RNaseA and Proteinase K and reverse-crosslinked at 65°C overnight. DNA was phenol/chloroform extracted and precipitated using tRNA and glycogen as carriers. Purified ChIP DNA was used as template for qPCR using the primers corresponding to telomeric repeats and *Gapdh*. For re-ChIP, the immunoprecipitated chromatin complexes from first ChIP were eluted twice from the Protein A Sepharose, each with 100 μl 10 mM DTT at 37°C for 30 min. The eluted product was then diluted 20-fold with the sonication buffer (20 mM Tris pH 8.0, 2 mM EDTA, 150 mM NaCl, 0.1% SDS, 1% Triton X-100 and protease inhibitors) and preceded with second IP. DNA primers for ChIP include:

Telomere primers: 5′-GGTTTTTGAGGGTGAGGG TGAGGGTGAGGGTGAGGGT-3′ and

5′-TCCCGACTATCCCTATCCCTATCCCTATCCCT ATCCCTA-3′ and

GAPDH primers: 5′-AGAGAGGGAGGAGGGGAA ATG-3′ and 5′-AACAGGGAGGAGCAGAGAGCAC-3′.

Northern blot analysis

Total RNA was isolated using RNeasy as described above and run on 1% agarose gel with formalydehyde. Following gel electrophoresis, RNA was transferred onto Hybond N+ nitrocellulose membrane. The membrane was baked and subjected to hybridization analysis with either α-32p-labeled $(TTAGGG)_4$ telomere probe. Signal intensities were analyzed with Typhoon PhosphoImager System and ImageQuant software.

RESULTS

H3.3 deficiency reduces H3K9me3 levels and causes loss of chromatin repression at telomeres

While H3.3 lysine (K)4 methylation is important for maintaining transcriptional memory (1), how H3.3 facilitates heterochromatin assembly at telomeres is unclear (32). To address this question, we generated *H3f3a* or *H3f3b* null mouse ESCs (29). These cells in particular *H3f3b*$^{-/-}$ cells show a significant reduction in H3.3 protein levels relative to WT cells (Figure 1A), suggesting that *H3f3b* encodes for a larger proportion of H3.3 protein expression. The reduced endogenous H3.3 expression, particularly in *H3f3b*$^{-/-}$ ESCs provides an ideal model to examine the role of H3.3 in heterochromatin assembly at telomeres. Chromatin immunoprecipitation (ChIP)-qPCR of telomere repeats (Figure 1B and Supplementary Figure S1A) was performed and validated by dot blot analysis (Supplementary Figure S1B–D). In WT ESCs, the positive control Histone H3 ChIP-qPCR shows a high level of enrichment of H3 at telomeres (Supplementary Figure S1A). These cells also show a strong enrichment of H3.3, ATRX and two heterochromatin marks, H3K9me3 and H4K20me3, at telomeres (Figure 1B and Supplementary Figure S1A). As expected, H3.3, but not ATRX, H3K9me3 and H4K20me3, is also enriched at the transcriptionally active *Gapdh* locus (Supplementary Figure S1A). However, it is remarkable that ChIP-qPCR in *H3f3a*$^{-/-}$ and *H3f3b*$^{-/-}$ ESCs shows not only a significant reduction in H3.3 enrichment

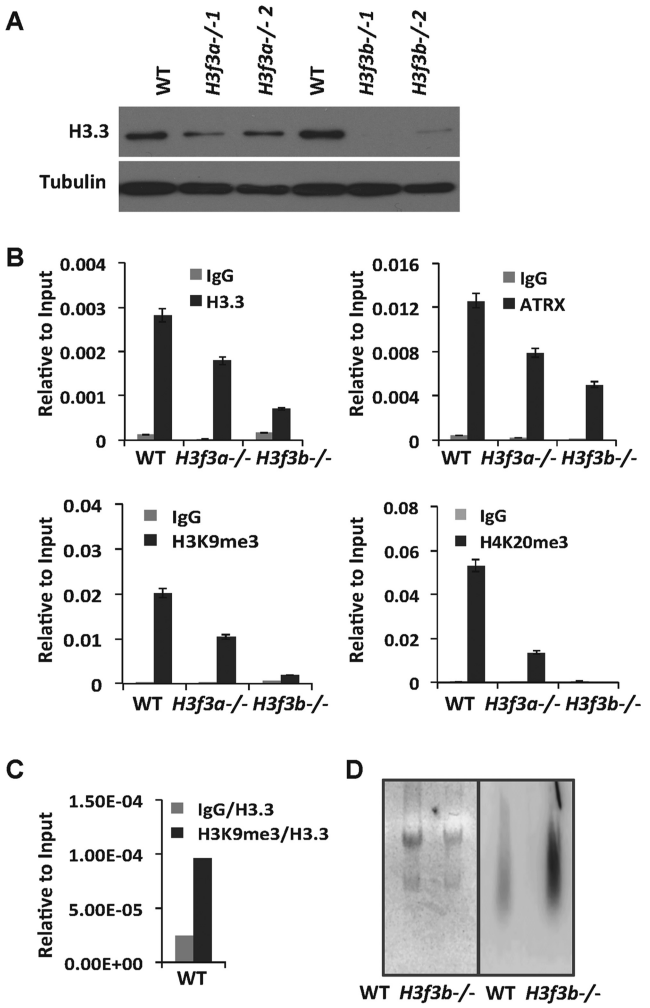

Figure 1. H3.3 deficiency results in a compromised heterochromatic state at telomeres in mouse ESCs. (**A**) Western blot analyses using antibodies against histone H3.3 and alpha tubulin. H3.3A and H3.3B protein levels are reduced by 30% and 80% in *H3f3a*$^{-/-}$ and *H3f3b*$^{-/-}$ mouse ESC clones, respectively. Alpha tubulin was used as loading control for normalization. (**B**) ChIP-qPCR analysis of H3.3, ATRX, H3K9me3 and H4K20me3 at telomeres in wild-type (WT), *H3f3a*$^{-/-}$ and *H3f3b*$^{-/-}$ ESCs. Chromatin was fixed, sonicated and subjected to ChIP with specific antibodies. Each ChIP was performed with 2 μg of antibody pre-bound to Protein A Sepharose. The ChIP products were eluted, purified and subjected to real-time PCR analyses with relevant DNA primers. Y-axis represents relative enrichment over 'Input' and Mean ± SD of three replicate experiments are shown. (**C**) Sequential ChIP-qPCR analysis of H3.3 enrichment in K9me3 at telomeres. H3K9me3 was first ChIPed, followed by re-ChIP of H3.3 from the eluted chromatin-enriched with H3.3K9me3. The ChIP products were eluted, purified and subjected to real-time PCR analyses with relevant DNA primers. (**D**) Total RNA was purified and subjected to agarose gel electrophoresis and Northern blot analysis using γ-^{32}pATP labeled TTAGGG DNA probe. An increase (by three-fold) in TERRA expression level was detected in *H3f3b*$^{-/-}$ mouse ESC clones (right panel). The levels of total RNA loaded are shown (left panel).

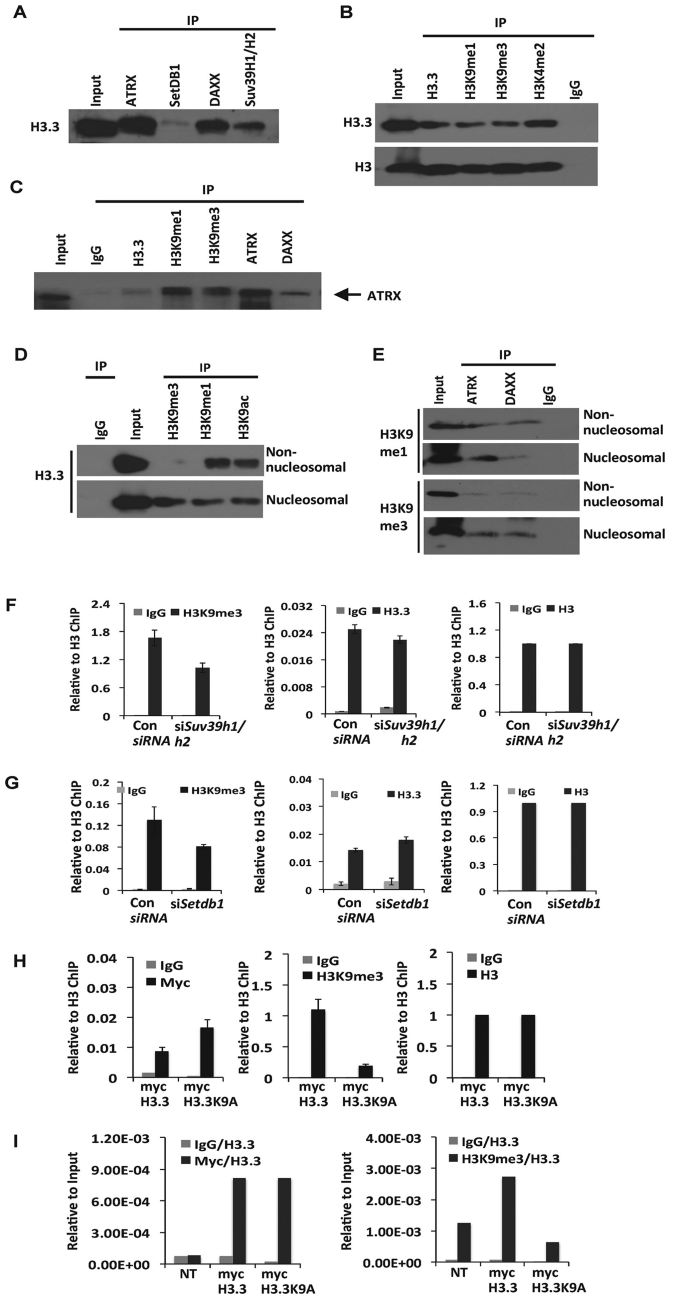

Figure 2. H3.3 is targeted for K9me3 in mouse ESCs. (**A**) Protein immunoprecipitations with antibodies against ATRX, DAXX, SETDB1 and SUV39H1/2, followed by western blot analysis with an antibody against H3.3. (**B**) Protein immunoprecipitations with antibodies against H3.3, H3K9me1, H3K9me3 and H3K4me3, followed by western blot analysis with antibodies against H3.3 and H3, respectively. (**C**) Protein immunoprecipitations with antibodies against H3.3, H3K9me1, H3K9me3, ATRX and DAXX, followed by western blot analysis with an antibody against ATRX. (**D** and **E**) Protein immunoprecipitation was performed in both non-nucleosomal and nucleosomal lysates. In (D), antibodies against H3K9me1, H3K9me3 and H3K9ac were used in protein immunoprecipitation, followed by western blot analysis with an antibody against H3.3. In (E), antibodies against ATRX and DAXX were used in protein immunoprecipitation, followed by western blot analysis with antibodies against H3K9me1 and H3K9me3, respectively. (**F** and **G**) ChIP-qPCR analyses of H3K9me3, H3.3 and H3 at the telomeres. The results show reduced levels of H3K9me3 and H3.3 at the telomeres in *Suv39h1/Suv39h2* (F) and *Setdb1* (G) siRNA-depleted ESCs. 'Con' refers to control siRNA. Y-axis represents relative enrichment after normalization against H3 ChIP. (**H**) ChIP/qPCR of H3K9me1, H3K9me3 and H3 at telomeres in *H3f3b*$^{-/-}$ ESCs expressing either myc-H3.3 (H3.3) or a myc-H3.3K9A mutant (H3.3K9A). Y-axis represents relative enrichment after normalization against H3 ChIP. Cells transfected with myc-H3.3 show a greater increase in H3K9me3, compared to cells transfected with myc-H3.3K9A mutant. (**I**) ChIP/re-ChIP qPCR of myc/H3.3 and H3.3/H3K9me3 at telomeres in *H3f3b*$^{-/-}$ ESCs (NT, non-transfected control) with overexpression of either myc-H3.3 (H3.3) or mutant myc-H3.3K9A (H3.3K9A). (Left) Cells were ChIPed with IgG or anti-Myc antibody, followed by re-ChIPed with an antibody against H3.3. (Right) Cells were ChIPed first with IgG or anti-H3K9me3 antibody, followed by re-ChIPed with an antibody against H3.3. Cells transfected with myc-H3.3 show a greater increase in H3K9me3/H3.3 ChIP/re-ChIP, compared to cells transfected with myc-H3.3K9A mutant.

at telomeres, but also in the levels of ATRX and of two important hallmarks of heterochromatin, namely H3K9me3 and H4K20me3 (Figure 1B). Dot blot analysis (Supplementary Figure S1B–D) confirms a similar reduced pattern of H3.3, ATRX, H3K9me3 and H4K20me3 at telomeres in *H3f3a*$^{-/-}$ and *H3f3b*$^{-/-}$ ESCs. The loss of H3K9me3 at telomeres in H3.3 deficient cells suggests that H3.3 provides as an important substrate for H3K9 trimethylation at telomeres, and that the reduced levels of ATRX binding and telomeric heterochromatin marks (*i.e.* H4K20me3) may be a result of the loss of H3.3K9me3 mark. Consistent with this idea, we show co-enrichment of H3K9me3 and H3.3 at telomeres in a sequential ChIP-qPCR assay in WT cells. In this assay, H3K9me3-enriched chromatin was first ChIPed, eluted, then subjected to a second round of ChIP using an antibody to H3.3 (Figure 1C). In addition, we show in *H3f3b*$^{-/-}$ ESCs that low levels of H3.3 lead to increased levels of the telomeric Terra transcripts (33,34) (Figure 1D) which reflects a compromised heterochromatin state at the telomeres, and agrees with the increase of Terra transcription found in ATRX-null ESCs that fail to load H3.3 at telomeres (10). Together, these findings indicate H3.3 provides as an important substrate for H3K9 trimethylation and the importance of H3.3K9me3 in facilitating heterochromatin assembly, as indicated by the reduced levels of ATRX and H4K20me3 at the telomeres, accompanied with an increase in TERRA transcript level.

H3.3 is targeted for K9 trimethylation

Previous mouse knockout studies have demonstrated the importance of SUV39H enzymes as HMTases in maintaining H3K9me3 and chromatin repression at telomeres (32). To examine the possible involvement of these SUV39H enzymes in mediating H3.3K9 trimethylation, we performed protein immunoprecipitation assays to assess interaction of H3.3 with SUV39H1 and SUV39H2 (Figure 2A). In the assays, we have also included SETDB1 that plays a role in promoting H3K9 methylation in various genomic regions (32,35–39). H3.3 displays a clear interaction not only with SUV39H1 and SUV39H2, but also with SETDB1 (Figure 2A). This indicates that H3.3 protein (that associates with ATRX/DAXX chaperone complex) could potentially be targeted for K9 methylation, and provides as a heterochromatic mark at the telomeres. To investigate this, protein immunoprecipitations were performed with antibodies against

H3K9 mono (H3K9me1) and trimethylation (H3K9me3), followed by western blot analyses with antibodies against H3.3 and H3 (Figure 2B). In both H3K9me1 and H3K9me3 immunoprecipitates, we detect the presence of H3.3 (Figure 2B). As controls, H3.3 is also detected in H3K4me3 immunoprecipitate, and H3 in H3K4me3, H3K9me1 and H3K9me3 immunoprecipitates (Figure 2B). We have also performed western blot analyses with an antibody against ATRX and detect the presence of ATRX in H3K9me1 and H3K9me3 immunoprecipitates (Figure 2C). These data indicate that H3.3 associated with ATRX complex can be targeted for K9 methylation, specifically K9 mono- and trimethylation.

Previous studies have suggested a step-wise process for H3K9 trimethylation involving a monomethylation step prior to di- or trimethylation (4,40,41). K9 monomethylation of H3/H3.3 prior to incorporation into chromatin, may conceivably influence the ability of SETDB1, SUV39H1 and SUV39H2 to promote K9 trimethylation after chromatin loading, including at telomeres (4). Indeed, a recent study shows that H3K9me1 directed by PRDM3 and PRDM16 mono methyltransferases is further converted to H3K9me3 by the SUV39H1 and SUV39H2 enzymes to facilitate heterochromatin assembly at pericentric DNA (40). To examine the possibility that H3.3 may be subjected to a stepwise K9 methylation, we performed protein immunoprecipitation with antibodies against H3K9me1 and H3K9me3 in both non-nucleosomal and nucleosomal (chromatin bound) lysates. In line with a stepwise model, we detect K9me1 on both non-nucleosomal (non-chromatin bound) and nucleosomal (chromatin bound) H3.3, while K9me3 is detected predominantly on nucleosomal H3.3 (Figure 2D). We also detect H3K9me1 and H3K9me3 in ATRX and DAXX immunoprecipitates- H3K9me1 is found mainly from the non-nucleosomal fraction, while, H3K9me3 from the nucleosomal fraction (Figure 2E). These findings indicate that H3.3 may be targeted for K9 monomethylation prior to being subjected to K9 trimethylation. Our results support previous observation (4,40,41) that non-nucleosomal H3.3 can be pre-modified in a non-nucleosomal form (K9me1) prior to a further modification of K9 by HMTases to form K9me3 at heterochromatic region (4).

To investigate the importance of H3.3 K9 trimethylation, we performed siRNA-mediated depletion of SETDB1 and SUV39H1/H2 in ESCs (Supplementary Figure S2A and B), given both of these HMTases interact with H3.3, and their roles in directing H3K9 methylation. Reduced levels of K9me3 on H3.3 were detected in SETDB1 and SUVAR39H1/H2 depleted cells (Supplementary Figure S2C). A reduction of K9me1 was also found in SETDB1 depleted cells, in consistent with the role of SETDB1 in promoting H3K9 monomethylation. Next, we performed ChIP/qPCR analysis to determine the level of H3K9 trimethylation at telomeres in SETDB1 and SUVAR39H1/H2 depleted cells (Figure 2F and G). The siRNA mediated depletion of *Setdb1* and *Suvar39h1/h2* led to a reduction of H3K9me3 at the telomeres. These findings indicate SETDB1 and SUV39H1/H2 act as HMTases that trimethylate H3.3 to establish the H3.3K9me3 mark at telomeres, consistent with the roles of H3.3 and H3K9me3 in directing heterochromatin assembly at the telomeres (32,36,42).

H3.3K9me3 deficiency leads to a compromised heterochromatic state and chromatin integrity at telomeres in *H3f3b*$^{-/-}$ cells

We next investigated the importance of H3.3K9 in establishing the H3K9me3 mark at telomeres in a complementation study (Figure 2H). First, we expressed myc-tagged H3.3 and H3 in *H3f3b*$^{-/-}$ ESCs, respectively, followed by ChIP-qPCR analysis to determine levels of deposition and H3K9me3 at telomeres (Supplementary Figure S3). Following normalization by the levels of deposition at *Gapdh* gene promoter, myc-H3.3 is deposited at a higher level at the telomeres (compared to myc-H3) and the level of increase in H3K9me3 at telomeres is also higher in myc-H3.3 expressing cells. To further investigate the link of H3.3 deposition to H3K9me3 formation, we expressed a myc-tagged H3.3 or mutant myc-H3.3K9A (bearing a K9→A substitution) in *H3f3b*$^{-/-}$ ESCs followed by ChIP-qPCR analysis to determine levels of H3K9me3 at telomeres. *H3f3b*$^{-/-}$ ESCs expressing myc-H3.3 show a greater level of H3K9me3 at telomeres compared to cells expressing the myc-H3.3K9A mutant (Figure 2H). Additionally, sequential ChIP reveals a significant increase in co-enrichment of H3.3/H3K9me3 at telomeres in *H3f3b*$^{-/-}$cells expressing myc-H3.3 (Figure 2I). This indicates that expression of myc-H3.3 can restore H3K9me3 levels at the telomeres, whereas the myc-H3.3K9A mutant is unable to compensate for the loss of H3K9me3. This highlights the importance of H3.3 as a target for K9 trimethylation for the establishment of the heterochromatic mark at telomeres.

The importance of H3K9me3 for chromatin repression at telomeres (32) suggests that deficiency of H3.3 or H3.3K9me3 may affect telomere heterochromatin maintenance and thus, potentially increasing cell sensitivity to activities that induce chromatin disruption at the telomeres. However, we find that in *H3f3a*$^{-/-}$ and *H3f3b*$^{-/-}$ ESCs, neither telomeric DNA damage (assessed by positive staining of γ-H2AX at telomeres known as the telomere dysfunctional foci (TIF)) (Figure 3A and C) nor sister chromatid exchange (t-SCE; determined by CO-FISH) (Figure 3B; examples of t-SCE are shown in Supplementary Figure S4A and B) are increased under normal ESC growth conditions when compared to those in WT cells. This suggests that a reduced H3.3 or H3.3K9me3 level does not significantly affect telomere stability and cell function in a normal unperturbed condition. It agrees with the observation that ATRX null mouse ESCs that fail to deposit H3.3 at telomeres also do not show significant changes in TIF, t-SCE and cell function under an unperturbed condition (43). Nevertheless, it has been noted that ATRX null cells show an increased sensitivity toward DNA replication stress, and this has been demonstrated using DNA replication inhibitors and a G-quadruplex (G4) binding ligand (26,27,44). The function of ATRX in H3.3 deposition has been proposed to be essential for re-chromatinization upon recovery from replication stress and thus, chromatin disruption caused by these drugs at telomeres (26). To examine if a lack of H3.3 affects telomere function in a similar manner

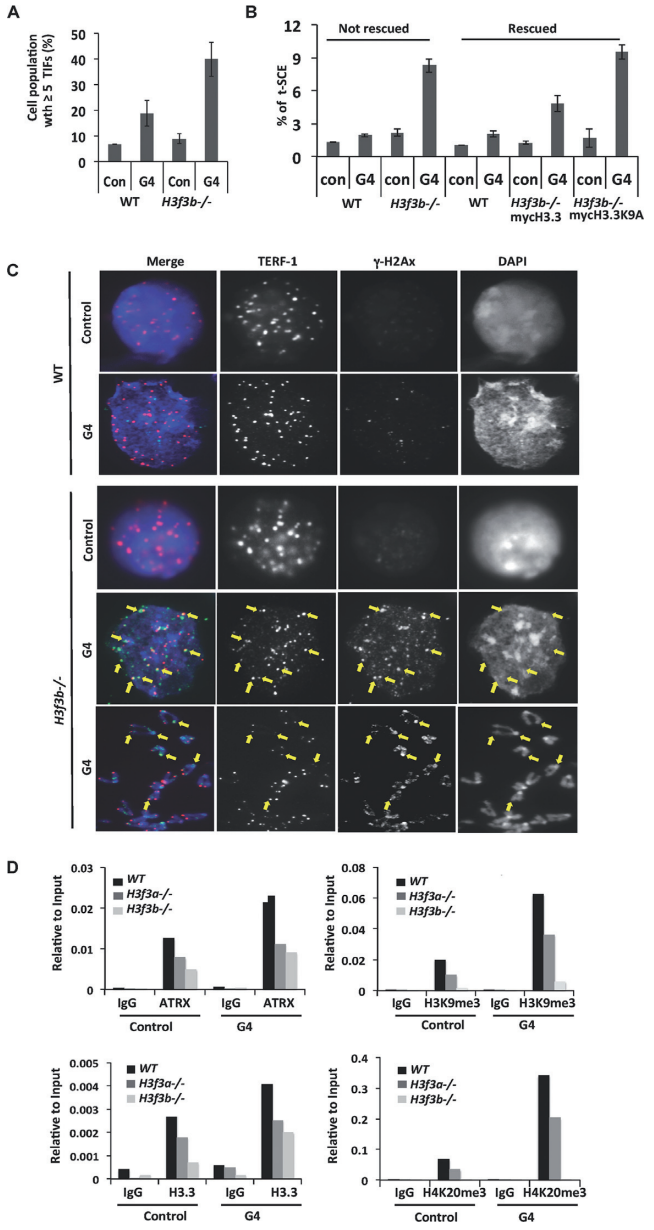

Figure 3. H3.3K9 is required for heterochromatin formation and chromatin integrity at telomeres in mouse ESCs. (**A**–**C**) WT and *H3f3b*$^{-/-}$ ESCs were subjected to with ('G4') or without ('Con') a 6-day treatment with 2 μM TMPYP4. Immunofluorescence (A and C) and CO-FISH (B; refer to Supplementary Figure S5 for examples) analyses were performed to detect TIF (telomeric foci with positive of γ-H2Ax staining) (A and C) and t-SCE (B). (A) *H3f3b*$^{-/-}$ ESCs show a greater increase cell population with ≥5 TIF per cell, compared to WT cells subjected to 6-day treatment with 2 μM TMPYP4 (examples of an increase in TIF formation are shown in (C)). Mean ± SD of three replicate experiments are shown. (B) *H3f3b*$^{-/-}$ cells show a greater increase in t-SCE, when compared to WT cells. And, an overexpression of WT myc-H3.3 ('rescue') in *H3f3b*−/− cells results in reduced t-SCE levels compared to overexpression of myc-H3.3K9 mutant. Y-axis represents an average number of t-SCE events per metaphase spread in a total of 35 cells examined. (**D**) ChIP analyses were performed using antibodies against ATRX, H3.3, H3K9me3 and H4K20me3, followed by qPCR analyses. Increased levels of ATRX, H3.3, H3K9me3 and H4K20me3 are found at telomeres in WT, *H3f3a*$^{-/-}$ and *H3f3b*$^{-/-}$ ESCs following 6 h TMPYP4 treatment (G4). Lower increases are detected in *H3f3a*$^{-/-}$ and *H3f3b*$^{-/-}$ cells. Y-axis represents relative enrichment to Input DNA.

to those in ATRX-null cells, we proceed to induce replication stress and chromatin disruption in H3.3-deficient cells. To avoid the high-levels of DNA damage induced by global replication inhibitors such as aphidicolin (APH), or drastic changes in H3.3 levels and histone post-translational modifications (Supplementary Figure S5A–C), we have treated cells with a low concentration of TMPYP4 (45). TMPYP4 is a ligand that binds and stabilizes a G4 DNA secondary structure that form at telomeres (46). When a G4 structure forms in the telomeric DNA template and is not resolved, it will impede the progression of the replication fork thus, inducing replication stress and chromatin disruption (46). In our assays, we choose to use TMPYP4 to induce replication stress because it is more specific to the telomeres than a global replication inhibitor such as aphidicholin. Compared to WT ESCs, TMPYP4 treatment of *H3f3b*$^{-/-}$ ESCs leads to an increase in telomeric DNA damage or TIF formation on both interphase and metaphase chromosomes (Figure 3A and C). TMPYP4 treatment of *H3f3b*$^{-/-}$ ESCs also induces an increase in t-SCE activity indicating telomere instability, nevertheless, at a low level (Figure 3B and Supplementary Figure S4A and B). Overexpression of myc-H3.3, but not the myc-H3.3K9A mutant, reduces t-SCE levels in these cells, indicating that a restoration of H3.3 supply and H3.3K9me3 represses t-SCE. C-circles are a specific marker of ALT activity (47), and we also quantitated C-circle formation in these cells (Supplementary Figure S6A). Compared to human ALT cancer cells, we detect only a modest increase of C-circle formation in *H3f3b*$^{-/-}$ cells after 6 days of treatment with TMPYP4 (Supplementary Figure S6A). This also agrees with the absence of the formation of ALT-associated PML bodies (APBs), indicating a lack of ALT induction in *H3f3b*$^{-/-}$ ESCs treated with TMPYP4 (Supplementary Figure S6B). It remains unknown if a prolonged period of TMPYP4 may induce a further increase in C-circles or APB formation, however, this could not be tested in *H3f3b*$^{-/-}$ ESCs as the 6 day TMPYP4 treatment promotes cellular differentiation in these cells. Together, our data show that cells deficient of H3.3 suffer greater levels of telomeric DNA damage and chromatin instability when telomeres are compromised by treatment with G4 ligands, and that we detect a phenotypic recovery with overexpression of H3.3 WT but not the H3.3K9 mutant proteins. These findings demonstrate the involvement of H3.3/H3.3K9 in the maintenance of telomeric chromatin integrity, in particular, during when telomere chromatin assembly is disturbed (11,12,32).

Given H3.3 loading can occur anytime during the cell cycle, it may support heterochromatin assembly at telomeric DNA following recovery from TMPYP4-induced replication stress and chromatin disruption. As such, it is possible that TMPYP4 treatment may induce ATRX-dependent H3.3 loading at telomere upon recovery in order to re-chromatinize the telomeres and to assemble a repressed chromatin state. In *H3f3b*$^{-/-}$ cells, a lack of H3.3 may result in a loss of H3.3K9me3 and chromatin repression, and this agrees with previous studies that show the importance of K9me3 binding of ATRX (48) and its interacting partner such as HP1 This loss in chromatin repression may ultimately lead to increases in DNA damage and t-SCE at telomeres (see Figure 3A–C). Consistent with these hy-

potheses, we detect increased levels of ATRX and H3.3 at telomeres in WT ESCs after treatment with a low level of TMPYP4, as indicated by ChIP/qPCR analyses (Figure 3D). These increases in the levels of ATRX and H3.3 binding at the telomeres in TMPYP4 treated cells are accompanied by up-regulated levels of heterochromatic marks including H3K9me3 and H4K20me3. Similar increases are detected in *H3f3b*$^{-/-}$ cells, however, at much lower levels compared to those in WT cells. The enhanced ATRX binding and H3.3 loading may be required for nucleosome re-assembly and heterochromatin formation at telomeres as cells recover from TMPYP4-induced chromatin disruption. In *H3f3b*$^{-/-}$ cells, the limited increase in ATRX, H3K9me3 and H4K20me3 suggests that H3.3 deficiency may impact ATRX binding and thus, heterochromatin assembly at telomeres.

To further investigate the importance of H3.3 in telomeric heterochromatin assembly, we next examine the impact of H3.3 deficiency in cells experiencing replication stress and chromatin disruption induced as a result of siRNA depletion of *Asf1a* and *Asf1b* (49) (Supplementary Figures S7 and S8). ASF1 (ASF1 a and ASF1b) are histone chaperones that play an essential role in nucleosome assembly and histone recycling during replication and loss of ASF can uncouple chromatin assembly from DNA replication (50). It has been shown that loss of ASF1 in cells can induce DNA damage at telomeres and ALT (49). Consistent with the role of ASF1 in DNA replication and nucleosome assembly, we have detected γ-H2AX on chromosome arms, and high levels of telomeric DNA damage or TIF formation following siRNA depletion of *Asf1a/1b* in both WT and *H3f3b*$^{-/-}$ ESCs (Figure 4A and B*;* examples of TIFs in interphase cells are shown in Supplementary Figure S8A and B). However, compared to WT ESCs, H3.3 deficient *H3f3b*$^{-/-}$ ESCs show a greater increase in the proportion of cells with ≥5 positive γ-TIF foci per cell following *Asf1a/1b* siRNA depletion (Figure 4A and B). The presence of TIF is prominent in both interphase and metaphase nucleic (Figure 4A and B and Supplementary Figure S8A and B). These *H3f3b*$^{-/-}$ cells also show a slight increase in t-SCE level following *Asf1a/1b* siRNA depletion (Figure 4B). These findings indicate that *H3f3b*$^{-/-}$ ESCs also show an increased sensitivity to replication stress and chromatin disruption induced by loss of ASF1, as seen in cells subjected to treatment with TMPYP4.

Considering the role of ATRX in loading H3.3 at telomeres, we also investigate if cells depleted of ATRX expression are sensitive to replication stress and chromatin disruption induced by a siRNA depletion of *Asf1a* and *Asf1b*. Indeed, a combined *Atrx* and *Asf1a/b* siRNA depletion results in greater levels of TIF and t-SCE compared to those induced by *Asf1* siRNA depletion alone in WT ESCs (Figure 4A and B). However, in *H3f3b*$^{-/-}$ ESCs, the levels of increase in TIF and t-SCE induced by a combined *Atrx* and *Asf1a/b* siRNA depletion are comparable to those induced by a single *Asf1a/1b* siRNA-depletion. These increases in TIF and t-SCE in *H3f3b*$^{-/-}$ ESCs are also similar to those detected in WT ESCs subjected to a combined *Atrx* and *Asf1a/b* siRNA depletion. These data agree with the finding that ATRX and H3.3 act in the same pathway in maintaining telomeric chromatin assembly. It is, however, interesting

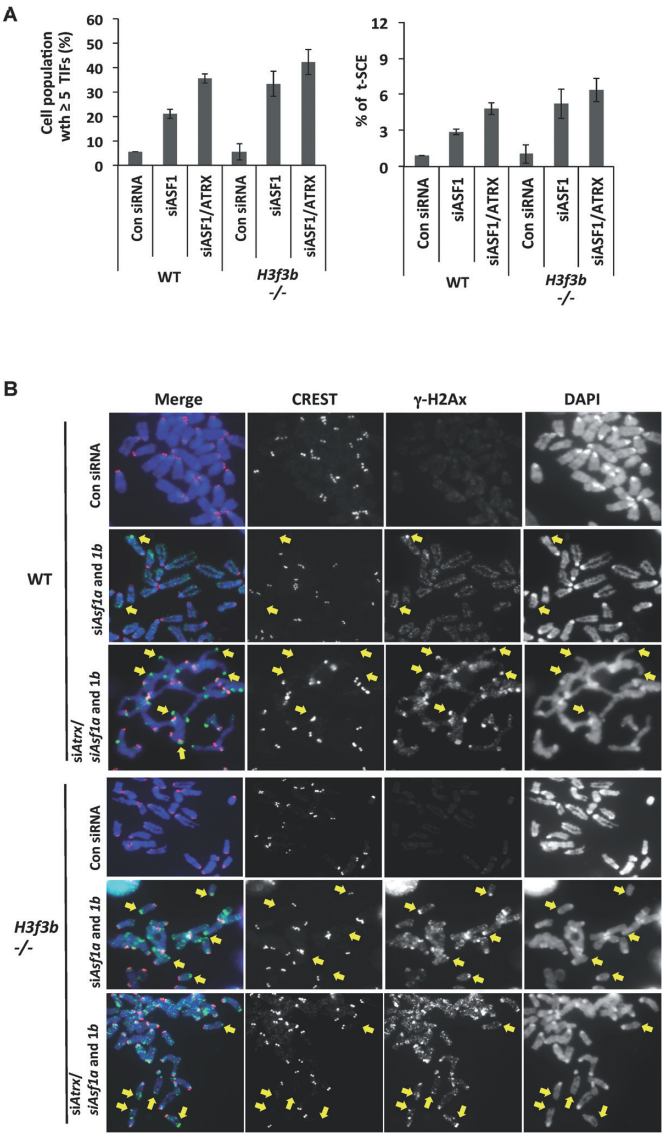

Figure 4. H3.3 deficient ESCs are sensitive to the induction of nucleosome disruption. Immunofluorescence analysis was performed to detect the presence of TIF (indicated by positive γ-H2Ax staining at telomeres) following 96 h siRNA-depletion of either *Asf1a/b* alone or a combined *Atrx* and *Asf1a/b* in both WT and *H3f3b*$^{-/-}$ ESCs. (**A**) WT ESCs subjected to a combined *Atrx* and *Asf1a/b* siRNA depletion (for 96 h) show a much greater increase in cell population with ≥5 TIF per cell, compared to ESCs subjected to a single *Asf1a/b* siRNA depletion (for 96 h). In the *H3f3b*$^{-/-}$ background, cells subjected to a single *Asf1a/b* siRNA depletion show a comparable increase in the level of cell population with ≥5 TIF per cell when compared to cells subjected to a combined *Atrx* and *Asf1a/b* siRNA depletion. These levels of increase in TIF in *H3f3b*$^{-/-}$ cells are also similar to those detected in WT ESCs subjected to a combined *Atrx* and *Asf1a/b* siRNA depletion. Examples of TIF on metaphase chromosomes are shown in (**B**). In parallel, CO-FISH was performed to assess t-SCE activity (A). In WT background, a combined siRNA depletion of *Atrx* and *Asf1a/b* results in a further increase in t-SCE compared to a single *Asf1a/b* siRNA depletion alone. In the *H3f3b*$^{-/-}$ background, cells subjected to a single *Asf1a/b* siRNA depletion show a comparable increase in t-SCE when compared to cells subjected to a combined *Atrx* and *Asf1a/b* siRNA depletion. The levels of increase in t-SCE in *H3f3b*$^{-/-}$ cells subjected to a single *Asf1a/b* siRNA depletion are also similar to that detected in WT ESCs subjected to a combined *Atrx* and *Asf1a/b* siRNA depletion.

to note that the t-SCE levels remain relatively low despite the significant increases in γ-H2AX levels at the telomeres in *Asf1* and *Atrx* and *Asf1a/1b* siRNA depleted cells, respectively (Figure 4A and B). This suggests that additional mechanisms may operate to suppress t-SCE activity even if telomeres suffer a high level of DNA damage in ESCs. A much longer period of *Asf1a/1b* siRNA depletion may be required for further upregulation of t-SCE in *H3f3b*$^{-/-}$ cells, however, this is not possible to test as *H3f3b*$^{-/-}$ ESC cells undergo cellular differentiation 96 h after ASF1 depletion (data not shown). Together, our data indicate that H3.3 deficiency (or loss of ATRX mediated H3.3 loading) renders cells more sensitive to replication stress and chromatin disruption induced by ASF1 depletion, in a like manner to those induced by TMPYP4 treatment.

DISCUSSION

While the role of K4 trimethylation of H3.3 in maintaining transcriptional memory at active chromatin is well described (1,2), little was known regarding how H3.3 facilitates the assembly of a heterochromatic state. Using H3.3-deficient ESCs, complementation studies and mutational analyses, we now demonstrate that H3.3 availability is essential for maintenance of a heterochromatic state through H3.3K9 trimethylation and ATRX recruitment to telomeres, and thereby for proper telomere function. Our results are consistent with studies showing the importance of H3K9me3 as a docking site for ATRX (48,51) and their roles in maintaining transcription repression at telomeres.

It has been well documented that SETDB1, SUV39H1 and SUV39H2 are important HTMases that promote H3K9 methylation (32,42). Here, we show that H3.3 interacts with SETDB1, SUV39H1 and SUV39H2, and that siRNA depletion of *Setdb1* and *Suvar39h1/h2* result in a reduced level of K9me3 on H3.3 and also a decrease in H3K9me3 level at the telomeres. These data agree with the previous findings that gene knockouts of *Suvar39h1* and *Suvar39h2* affect H3K9 trimethylation and chromatin repression at the telomeres. The role of SETDB1 at the telomere is less well defined, however, it has been reported to form complex with RIF1 to promote heterochromatin assembly at the telomeric regions (42). Furthermore, SETDB1 has been shown to form a multimeric complex with SUVAR39H1/2 in heterochromatin maintenance (36). As future work, it will be interesting to determine if SETDB1 forms a multimeric complex with SUVAR39H1/H2 to direct heterochromatin assembly at telomeres. We also show that H3.3 can be pre-modified by K9me1 prior to further K9me3 by HTMases upon loading to, or after deposition into, chromatin. These findings agree with a previous observation that a minor proportion of H3.3 is monomethylated on K9, although it is predominantly di-methylated on this residue (4). Further investigation is required to determine whether pre-modification of H3.3 before chromatin deposition provides specificity for HMases (4,39) as part of a stepwise mechanism to regulate sequential K9 trimethylation of H3.3. Such a mechanism would conceivably be coupled to ATRX-mediated deposition of H3.3 and the maintenance of a heterochromatic state at telomeres and possibly at other genomic sites. Indeed, two recent reports have shown that ATRX-mediated H3.3 deposition is important for promoting H3K9me3 formation, heterochromatin propagation and transcription silencing at retrotransposons including endogenous retroviral sequences (ERVs) and imprinted genes (52,53). However, in another recent study, it is proposed that ATRX mediates heterochromatic silencing at intracisternal A particle retrotransposable sequences in a manner independent of H3.3 deposition (54). Despite the disparities, these studies show consistent involvement of SETDB1 and TRIM28/KAP1 (KRAB-associated protein-1) in ATRX-mediated promotion of H3K9me3 formation and heterochromatic silencing at the retrotransposons (52,54). SETDB1 and TRIM28 have also been implicated in heterochromatin maintenance at imprinted genes in previous studies (55,56). A recent study has also identified the role of SUVAR39H1/2 in maintaining H3K9me3 marks and transcription silencing at intact ERVs and long interspersed nuclear elements (LINEs) (57). Taken together these findings, the functions of ATRX and H3.3 in directing H3K9me3 formation and heterochromatin assembly may involve the formation of a multimeric complex comprising of SETDB1, SUVAR39H1/2, TRIM28 and possibly others. Further investigations are needed to fully elucidate how ATRX/H3.3 may function as a complex to direct heterochromatin assembly and maintenance at the telomeres, imprinted genes and these retrotransposable repeats, in particular, how ATRX interacts with SETDB1 and SUVAR39H1/2 to mediate a stepwise K9 methylation on H3.3.

Here, we have also provided evidence for the importance of ATRX and H3.3 in response to replication stress at the telomeres. We show that increase of replication stress and chromatin disruption by treatment with TMPYP4 leads to an enhanced recruitment of ATRX and H3.3 and increases in H3K9me3 and H4K20me3 levels at telomeres. These data agree with a model where ATRX and H3.3 may be recruited as a response to nucleosome disruption in order to re-chromatinize telomeric DNA and assemble heterochromatin (Figure 5). It is likely that this ability to maintain heterochromatin and telomeric chromatin integrity is compromised in H3.3-deficient cells. Indeed, this is reflected in the increased sensitivity of *H3f3b*$^{-/-}$ cells and those depleted ATRX to replication stress and chromatin disruption induced by TMPYP4 or ASF1 depletion; these H3.3 deficient cells and cells defective in H3.3 deposition (due to a loss of ATRX function) suffer a greater incidence of telomeric DNA damage and t-SCE. Importantly, expression of WT H3.3 (but not the H3.3K9A mutant) partially restores H3K9me3 heterochromatin mark and reduces t-SCE in *H3f3b*$^{-/-}$ cells. These findings support our argument that H3.3 provides for the heterochromatic H3K9me3 mark and agree with the postulation that H3.3 acts as a 'replacement histone' at disrupted nucleosomal sites such as actively transcribed regions or damaged sites (28,58,59).

One important question remaining and to be further investigated is whether telomeres suffer significant chromatin disruption during normal cell cycle progression. This is possible given that G-rich telomeric repeats tend to form G4 structures (45) and G4-enriched sites are commonly predicted to be depleted or disrupted in nucleosome assembly (60,61). Indeed, telomeric repeats inherently disfavor nucle-

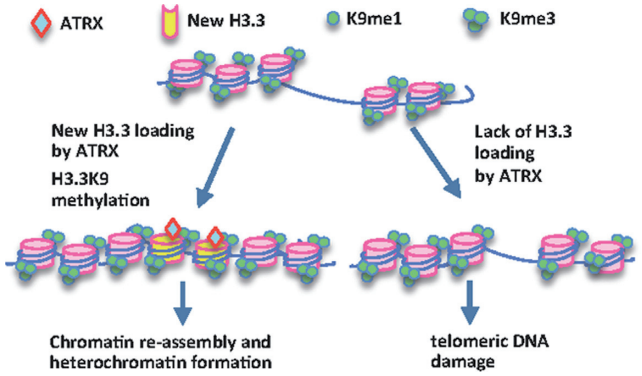

Figure 5. A model depicting H3.3 loading by ATRX to establish heterochromatin at telomeres. At nucleosomal disrupted sites such as those that form as a consequence of replication stall, transcription and nucleosomal dysfunction at telomeric repeats, ATRX loads H3.3 to facilitate re-chromatinization of DNA. H3.3 can be mono-methylated prior to its loading and K9 trimethylation at telomeres. This H3.3K9me mark is essential for chromatin repression at telomeres. In the absence of ATRX and H3.3, there will be prolonged nucleosomal disruption at these sites within the telomeric repeats. This may consequently lead to chromatin de-repression and damage at telomeres.

osome assembly (62). Moreover, transcription that occurs at these repeats can also cause chromatin disruption (33,34). These disrupted sites at telomeric repeats may be the driving factor that promotes H3.3 deposition by ATRX (Figure 5). H3.3 nucleosomes then provide targets for H3K9 trimethylation to allow heterochromatin assembly and to establish transcription silencing. In the event of a deficiency in H3.3 or ATRX, cells may experience improper chromatin assembly, a reduced level of H3.3K9me3 and loss of chromatin repression, indicated by the increases in Terra transcription. This may eventually induce DNA damage and repair by t-SCE. Finally, in line with these arguments, we propose that adequate and non-limiting levels of H3.3 and H3.3K9me3 are essential for the establishment of heterochromatin at telomeres. We also postulate that H3.3K9me3 may serve as a crucial chromatin mark for heterochromatin formation at other genomic sites.

SUPPLEMENTARY DATA

Supplementary Data are available at NAR Online.

FUNDING

National Health and Medical Research Council [NHMRC; ID #APP1031866] of Australia; Cancer Council of Victoria, Australia Postgraduate Scholarship [to F.T.M.C.]; Australia Research Council (ARC) Future Fellowship Award [to L.H.W.; ID #FT140100128]. Funding for open access charge: NHMRC; ARC, Australia.
Conflict of interest statement. None declared.

REFERENCES

1. Ahmad,K. and Henikoff,S. (2002) The histone variant H3.3 marks active chromatin by replication-independent nucleosome assembly. *Mol. Cell*, **9**, 1191–1200.
2. McKittrick,E., Gafken,P.R., Ahmad,K. and Henikoff,S. (2004) Histone H3.3 is enriched in covalent modifications associated with active chromatin. *Proc. Natl. Acad. Sci. U.S.A.*, **101**, 1525–1530.
3. Tagami,H., Ray-Gallet,D., Almouzni,G. and Nakatani,Y. (2004) Histone H3.1 and H3.3 complexes mediate nucleosome assembly pathways dependent or independent of DNA synthesis. *Cell*, **116**, 51–61.
4. Loyola,A., Bonaldi,T., Roche,D., Imhof,A. and Almouzni,G. (2006) PTMs on H3 variants before chromatin assembly potentiate their final epigenetic state. *Mol. Cell*, **24**, 309–316.
5. Schwartz,B.E. and Ahmad,K. (2005) Transcriptional activation triggers deposition and removal of the histone variant H3.3. *Genes Dev.*, **19**, 804–814.
6. Ng,R.K. and Gurdon,J.B. (2008) Epigenetic memory of an active gene state depends on histone H3.3 incorporation into chromatin in the absence of transcription. *Nat. Cell Biol.*, **10**, 102–109.
7. Chen,P., Zhao,J., Wang,Y., Wang,M., Long,H., Liang,D., Huang,L., Wen,Z., Li,W., Li,X. *et al.* (2013) H3.3 actively marks enhancers and primes gene transcription via opening higher-ordered chromatin. *Genes Dev.*, **27**, 2109–2124.
8. Drane,P., Ouararhni,K., Depaux,A., Shuaib,M. and Hamiche,A. (2010) The death-associated protein DAXX is a novel histone chaperone involved in the replication-independent deposition of H3.3. *Genes Dev.*, **24**, 1253–1265.
9. Lewis,P.W., Elsaesser,S.J., Noh,K.M., Stadler,S.C. and Allis,C.D. (2010) Daxx is an H3.3-specific histone chaperone and cooperates with ATRX in replication-independent chromatin assembly at telomeres. *Proc. Natl. Acad. Sci. U.S.A.*, **107**, 14075–14080.
10. Goldberg,A.D., Banaszynski,L.A., Noh,K.M., Lewis,P.W., Elsaesser,S.J., Stadler,S., Dewell,S., Law,M., Guo,X., Li,X. *et al.* (2010) Distinct factors control histone variant H3.3 localization at specific genomic regions. *Cell*, **140**, 678–691.
11. Wong,L.H., Ren,H., Williams,E., McGhie,J., Ahn,S., Sim,M., Tam,A., Earle,E., Anderson,M.A., Mann,J. *et al.* (2009) Histone H3.3 incorporation provides a unique and functionally essential telomeric chromatin in embryonic stem cells. *Genome Res.*, **19**, 404–414.
12. Wong,L.H., McGhie,J.D., Sim,M., Anderson,M.A., Ahn,S., Hannan,R.D., George,A.J., Morgan,K.A., Mann,J.R. and Choo,K.H. (2010) ATRX interacts with H3.3 in maintaining telomere structural integrity in pluripotent embryonic stem cells. *Genome Res.*, **20**, 351–360.
13. Chang,F.T., McGhie,J.D., Chan,F.L., Tang,M.C., Anderson,M.A., Mann,J.R., Andy Choo,K.H. and Wong,L.H. (2013) PML bodies provide an important platform for the maintenance of telomeric chromatin integrity in embryonic stem cells. *Nucleic Acids Res.*, **41**, 4447–4458.
14. Law,M.J., Lower,K.M., Voon,H.P., Hughes,J.R., Garrick,D., Viprakasit,V., Mitson,M., De Gobbi,M., Marra,M., Morris,A. *et al.* (2010) ATR-X syndrome protein targets tandem repeats and influences allele-specific expression in a size-dependent manner. *Cell*, **143**, 367–378.
15. Wong,L.H. (2010) Epigenetic regulation of telomere chromatin integrity in pluripotent embryonic stem cells. *Epigenomics*, **2**, 639–655.
16. Heaphy,C.M., de Wilde,R.F., Jiao,Y., Klein,A.P., Edil,B.H., Shi,C., Bettegowda,C., Rodriguez,F.J., Eberhart,C.G., Hebbar,S. *et al.* (2011) Altered telomeres in tumors with ATRX and DAXX mutations. *Science*, **333**, 425.
17. Di Antonio,M., Biffi,G., Mariani,A., Raiber,E.A., Rodriguez,R. and Balasubramanian,S. (2012) Selective RNA versus DNA G-quadruplex targeting by in situ click chemistry. *Angew. Chem. Int. Ed. Engl.*, **51**, 11073–11078.
18. Heaphy,C.M., Subhawong,A.P., Hong,S.M., Goggins,M.G., Montgomery,E.A., Gabrielson,E., Netto,G.J., Epstein,J.I., Lotan,T.L., Westra,W.H. *et al.* (2011) Prevalence of the alternative lengthening of telomeres telomere maintenance mechanism in human cancer subtypes. *Am. J. Pathol.*, **179**, 1608–1615.
19. Jiao,Y., Shi,C., Edil,B.H., de Wilde,R.F., Klimstra,D.S., Maitra,A., Schulick,R.D., Tang,L.H., Wolfgang,C.L., Choti,M.A. *et al.* (2011) DAXX/ATRX, MEN1, and mTOR pathway genes are frequently altered in pancreatic neuroendocrine tumors. *Science*, **331**, 1199–1203.

20. de Wilde,R.F., Heaphy,C.M., Maitra,A., Meeker,A.K., Edil,B.H., Wolfgang,C.L., Ellison,T.A., Schulick,R.D., Molenaar,I.Q., Valk,G.D. *et al.* (2012) Loss of ATRX or DAXX expression and concomitant acquisition of the alternative lengthening of telomeres phenotype are late events in a small subset of MEN-1 syndrome pancreatic neuroendocrine tumors. *Mod. Pathol.*, **25**, 1033–1039.
21. Cheung,N.K., Zhang,J., Lu,C., Parker,M., Bahrami,A., Tickoo,S.K., Heguy,A., Pappo,A.S., Federico,S., Dalton,J. *et al.* (2012) Association of age at diagnosis and genetic mutations in patients with neuroblastoma. *JAMA*, **307**, 1062–1071.
22. Capurso,G., Festa,S., Valente,R., Piciucchi,M., Panzuto,F., Jensen,R.T. and Delle Fave,G. (2012) Molecular pathology and genetics of pancreatic endocrine tumours. *J. Mol. Endocrinol.*, **49**, R37–R50.
23. Lovejoy,C.A., Li,W., Reisenweber,S., Thongthip,S., Bruno,J., de Lange,T., De,S., Petrini,J.H., Sung,P.A., Jasin,M. *et al.* (2012) Loss of ATRX, genome instability, and an altered DNA damage response are hallmarks of the alternative lengthening of telomeres pathway. *PLoS Genet.*, **8**, e1002772.
24. Bower,K., Napier,C.E., Cole,S.L., Dagg,R.A., Lau,L.M., Duncan,E.L., Moy,E.L. and Reddel,R.R. (2012) Loss of wild-type ATRX expression in somatic cell hybrids segregates with activation of Alternative Lengthening of Telomeres. *PLoS One*, **7**, e50062.
25. Wu,G., Broniscer,A., McEachron,T.A., Lu,C., Paugh,B.S., Becksfort,J., Qu,C., Ding,L., Huether,R., Parker,M. *et al.* (2012) Somatic histone H3 alterations in pediatric diffuse intrinsic pontine gliomas and non-brainstem glioblastomas. *Nat. Genet.*, **44**, 251–253.
26. Clynes,D., Higgs,D.R. and Gibbons,R.J. (2013) The chromatin remodeller ATRX: a repeat offender in human disease. *Trends Biochem. Sci.*, **38**, 461–466.
27. Watson,L.A., Solomon,L.A., Li,J.R., Jiang,Y., Edwards,M., Shin-ya,K., Beier,F. and Berube,N.G. (2013) Atrx deficiency induces telomere dysfunction, endocrine defects, and reduced life span. *J. Clin. Invest.*, **123**, 2049–2063.
28. Schneiderman,J.I., Orsi,G.A., Hughes,K.T., Loppin,B. and Ahmad,K. (2012) Nucleosome-depleted chromatin gaps recruit assembly factors for the H3.3 histone variant. *Proc. Natl. Acad. Sci. U.S.A.*, **109**, 19721–19726.
29. Tang,M.C., Jacobs,S.A., Wong,L.H. and Mann,J.R. (2013) Conditional allelic replacement applied to genes encoding the histone variant H3.3 in the mouse. *Genesis*, **51**, 142–146.
30. Tang,M.C., Jacobs,S.A., Mattiske,D.M., Soh,Y.M., Graham,A.N., Tran,A., Lim,S.L., Hudson,D.F., Kalitsis,P., O'Bryan,M.K. *et al.* (2015) Contribution of the two genes encoding histone variant h3.3 to viability and fertility in mice. *PLoS Genet.*, **11**, e1004964.
31. Chan,F.L., Marshall,O.J., Saffery,R., Kim,B.W., Earle,E., Choo,K.H. and Wong,L.H. (2012) Active transcription and essential role of RNA polymerase II at the centromere during mitosis. *Proceedings of the National Academy of Sciences of the U.S.A.*, **109**, 1979–1984.
32. Garcia-Cao,M., O'Sullivan,R., Peters,A.H., Jenuwein,T. and Blasco,M.A. (2004) Epigenetic regulation of telomere length in mammalian cells by the Suv39h1 and Suv39h2 histone methyltransferases. *Nat. Genet.*, **36**, 94–99.
33. Azzalin,C.M., Reichenbach,P., Khoriauli,L., Giulotto,E. and Lingner,J. (2007) Telomeric repeat containing RNA and RNA surveillance factors at mammalian chromosome ends. *Science*, **318**, 798–801.
34. Schoeftner,S. and Blasco,M.A. (2008) Developmentally regulated transcription of mammalian telomeres by DNA-dependent RNA polymerase II. *Nat. Cell Biol.*, **10**, 228–236.
35. Kouzarides,T. (2007) Chromatin modifications and their function. *Cell*, **128**, 693–705.
36. Fritsch,L., Robin,P., Mathieu,J.R., Souidi,M., Hinaux,H., Rougeulle,C., Harel-Bellan,A., Ameyar-Zazoua,M. and Ait-Si-Ali,S. (2010) A subset of the histone H3 lysine 9 methyltransferases Suv39h1, G9a, GLP, and SETDB1 participate in a multimeric complex. *Mol. Cell*, **37**, 46–56.
37. Karimi,M.M., Goyal,P., Maksakova,I.A., Bilenky,M., Leung,D., Tang,J.X., Shinkai,Y., Mager,D.L., Jones,S., Hirst,M. *et al.* (2011) DNA methylation and SETDB1/H3K9me3 regulate predominantly distinct sets of genes, retroelements, and chimeric transcripts in mESCs. *Cell Stem Cell*, **8**, 676–687.
38. Peters,A.H., O'Carroll,D., Scherthan,H., Mechtler,K., Sauer,S., Schofer,C., Weipoltshammer,K., Pagani,M., Lachner,M., Kohlmaier,A. *et al.* (2001) Loss of the Suv39h histone methyltransferases impairs mammalian heterochromatin and genome stability. *Cell*, **107**, 323–337.
39. Loyola,A., Tagami,H., Bonaldi,T., Roche,D., Quivy,J.P., Imhof,A., Nakatani,Y., Dent,S.Y. and Almouzni,G. (2009) The HP1alpha-CAF1-SetDB1-containing complex provides H3K9me1 for Suv39-mediated K9me3 in pericentric heterochromatin. *EMBO Rep.*, **10**, 769–775.
40. Pinheiro,I., Margueron,R., Shukeir,N., Eisold,M., Fritzsch,C., Richter,F.M., Mittler,G., Genoud,C., Goyama,S., Kurokawa,M. *et al.* (2012) Prdm3 and Prdm16 are H3K9me1 methyltransferases required for mammalian heterochromatin integrity. *Cell*, **150**, 948–960.
41. Towbin,B.D., Gonzalez-Aguilera,C., Sack,R., Gaidatzis,D., Kalck,V., Meister,P., Askjaer,P. and Gasser,S.M. (2012) Step-wise methylation of histone H3K9 positions heterochromatin at the nuclear periphery. *Cell*, **150**, 934–947.
42. Dan,J., Liu,Y., Liu,N., Chiourea,M., Okuka,M., Wu,T., Ye,X., Mou,C., Wang,L., Wang,L. *et al.* (2014) Rif1 maintains telomere length homeostasis of ESCs by mediating heterochromatin silencing. *Dev. Cell*, **29**, 7–19.
43. Garrick,D., Sharpe,J.A., Arkell,R., Dobbie,L., Smith,A.J., Wood,W.G., Higgs,D.R. and Gibbons,R.J. (2006) Loss of Atrx affects trophoblast development and the pattern of X-inactivation in extraembryonic tissues. *PLoS Genet.*, **2**, e58.
44. Conte,D., Huh,M., Goodall,E., Delorme,M., Parks,R.J. and Picketts,D.J. (2012) Loss of Atrx sensitizes cells to DNA damaging agents through p53-mediated death pathways. *PLoS One*, **7**, e52167.
45. Maizels,N. and Gray,L.T. (2013) The G4 genome. *PLoS Genet.*, **9**, e1003468.
46. Bochman,M.L., Paeschke,K. and Zakian,V.A. (2012) DNA secondary structures: stability and function of G-quadruplex structures. *Nat. Rev. Genet.*, **13**, 770–780.
47. Henson,J.D., Cao,Y., Huschtscha,L.I., Chang,A.C., Au,A.Y., Pickett,H.A. and Reddel,R.R. (2009) DNA C-circles are specific and quantifiable markers of alternative-lengthening-of-telomeres activity. *Nat. Biotechnol.*, **27**, 1181–1185.
48. Eustermann,S., Yang,J.C., Law,M.J., Amos,R., Chapman,L.M., Jelinska,C., Garrick,D., Clynes,D., Gibbons,R.J., Rhodes,D. *et al.* (2011) Combinatorial readout of histone H3 modifications specifies localization of ATRX to heterochromatin. *Nat. Struct. Mol. Biol.*, **18**, 777–782.
49. O'Sullivan,R.J., Arnoult,N., Lackner,D.H., Oganesian,L., Haggblom,C., Corpet,A., Almouzni,G. and Karlseder,J. (2014) Rapid induction of alternative lengthening of telomeres by depletion of the histone chaperone ASF1. *Nat. Struct. Mol. Biol.*, **21**, 167–174.
50. Groth,A., Corpet,A., Cook,A.J., Roche,D., Bartek,J., Lukas,J. and Almouzni,G. (2007) Regulation of replication fork progression through histone supply and demand. *Science*, **318**, 1928–1931.
51. Iwase,S., Xiang,B., Ghosh,S., Ren,T., Lewis,P.W., Cochrane,J.C., Allis,C.D., Picketts,D.J., Patel,D.J., Li,H. *et al.* (2011) ATRX ADD domain links an atypical histone methylation recognition mechanism to human mental-retardation syndrome. *Nat. Struct. Mol. Biol.*, **18**, 769–776.
52. Elsasser,S.J., Noh,K.M., Diaz,N., Allis,C.D. and Banaszynski,L.A. (2015) Histone H3.3 is required for endogenous retroviral element silencing in embryonic stem cells. *Nature*, **522**, 240–244.
53. Voon,H.P., Hughes,J.R., Rode,C., De La Rosa-Velazquez,I.A., Jenuwein,T., Feil,R., Higgs,D.R. and Gibbons,R.J. (2015) ATRX plays a key role in maintaining silencing at interstitial heterochromatic loci and imprinted genes. *Cell Rep.*, **11**, 405–418.
54. Sadic,D., Schmidt,K., Groh,S., Kondofersky,I., Ellwart,J., Fuchs,C., Theis,F.J. and Schotta,G. (2015) Atrx promotes heterochromatin formation at retrotransposons. *EMBO Rep.*, **16**, 836–850.
55. Quenneville,S., Verde,G., Corsinotti,A., Kapopoulou,A., Jakobsson,J., Offner,S., Baglivo,I., Pedone,P.V., Grimaldi,G., Riccio,A. *et al.* (2011) In embryonic stem cells, ZFP57/KAP1 recognize a methylated hexanucleotide to affect chromatin and DNA methylation of imprinting control regions. *Mol. Cell*, **44**, 361–372.
56. Leung,D., Du,T., Wagner,U., Xie,W., Lee,A.Y., Goyal,P., Li,Y., Szulwach,K.E., Jin,P., Lorincz,M.C. *et al.* (2014) Regulation of DNA methylation turnover at LTR retrotransposons and imprinted loci by the histone methyltransferase Setdb1. *Proc. Natl. Acad. Sci. U.S.A.*, **111**, 6690–6695.

57. Bulut-Karslioglu,A., De La Rosa-Velazquez,I.A., Ramirez,F., Barenboim,M., Onishi-Seebacher,M., Arand,J., Galan,C., Winter,G.E., Engist,B., Gerle,B. *et al.* (2014) Suv39h-dependent H3K9me3 marks intact retrotransposons and silences LINE elements in mouse embryonic stem cells. *Mol. Cell*, **55**, 277–290.
58. Ray-Gallet,D., Woolfe,A., Vassias,I., Pellentz,C., Lacoste,N., Puri,A., Schultz,D.C., Pchelintsev,N.A., Adams,P.D., Jansen,L.E. *et al.* (2011) Dynamics of histone H3 deposition in vivo reveal a nucleosome gap-filling mechanism for H3.3 to maintain chromatin integrity. *Mol. Cell*, **44**, 928–941.
59. Adam,S., Polo,S.E. and Almouzni,G. (2013) Transcription recovery after DNA damage requires chromatin priming by the H3.3 histone chaperone HIRA. *Cell*, **155**, 94–106.
60. Halder,K., Halder,R. and Chowdhury,S. (2009) Genome-wide analysis predicts DNA structural motifs as nucleosome exclusion signals. *Mol. Biosyst.*, **5**, 1703–1712.
61. Wong,H.M. and Huppert,J.L. (2009) Stable G-quadruplexes are found outside nucleosome-bound regions. *Mol. Biosyst.*, **5**, 1713–1719.
62. Ichikawa,Y., Morohashi,N., Nishimura,Y., Kurumizaka,H. and Shimizu,M. (2014) Telomeric repeats act as nucleosome-disfavouring sequences in vivo. *Nucleic Acids Res.*, **42**, 1541–1552.